



Preparation on iron of a polypyrrole (PPy) electrode modified with copper by the electrochemical cementation process

L. MAKHLOUFI*, H. HAMMACHE, B. SAIDANI, N. AKILAL and Y. MALOUM

Laboratoire de Recherche en Electrochimie et Corrosion, Institut de Chimie Industrielle, Université de Béjaia, 06000 Béjaia, Algeria

(*author for correspondence, fax: +213 521 43 32, e-mail: l.makhloufi@netcourrier.com)

Received 18 August 1999; accepted in revised form 31 March 2000

Key words: cementation, electrocatalysis, iron, modified electrodes, polypyrrole

Abstract

Conducting polypyrrole electrodes obtained under galvanostatic electropolymerization on iron from aqueous solutions of pyrrole and oxalic acid were modified with copper particles using the electrochemical cementation process. The electrochemical response of these modified electrodes was compared to that of the 'unmodified' polymer electrode and also to that of bare metallic copper. The modified polypyrrole electrode showed noticeable enhancement for the rate of proton reduction.

1. Introduction

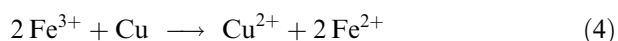
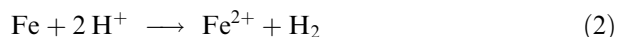
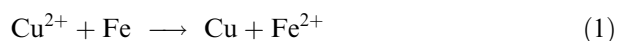
The study of conducting polymers, such as polypyrrole, polyaniline and polythiophene, and notably of electrodes modified by the incorporation of metal particles into the polymer film, has gained attention during the previous decade, because of their electrocatalytic properties [1–4]. These electrodes have enhanced the selectivity and the sensitivity of many interesting electroanalytical reactions and improved the function of amperometric biosensors and potentiometric sensors [5–7].

The metal particles usually used for the modification of polypyrrole films are platinum [2, 3], nickel complexes [8] and cobalt complexes [9]. These modified electrodes were generally electrosynthesized at inert electrodes such as platinum, glassy carbon or gold. This was done by (i) cyclic voltammetry, (ii) potential step technique, and (iii) chronoamperometry and/or chronopotentiometry, in the solution containing the suitably designed metal ions to be incorporated into the polymer film.

The first results describing a new procedure for preparation of a polypyrrole-modified electrode by the incorporation of copper into the polymer film are presented here. This process, called electrochemical cementation, is used for the first time to prepare a polymer modified electrode. Also, only recently [10], data on the fabrication of modified electrodes by the incorporation of group 4 transition metals (e.g., Cu) in the polymer film have been reported.

Cementation (or contact reduction) is the terminology for those spontaneous electrochemical reactions in which a metal ion in solution is reduced to the metal

with the concurrent oxidation of a more electropositive (or less noble) metal placed in the same solution. This type of reaction is heterogeneous in nature. This technology is usually applied to the recovery of noble metals from solutions and to the solution of heavy metal pollution problems [11–20]. The removal of copper by cementation on iron [21–23] and on lead [24] in aqueous acidic solutions has been widely studied. The reactions involved in copper cementation by iron in acidic solution are [25–27]:



Reactions 2 and 3 are responsible for the consumption of excess iron. Stoichiometrically, 1 kg of copper is precipitated by 0.88 kg of iron. In practice [28] 1.2 to 2.6 kg of iron are consumed when 1 kg of copper is formed. It was also established that Reactions 1 and 3 are concurrent and much faster than Reaction 2. Reaction 3 prevails when the Fe^{2+} ion concentration is low; for example, at the beginning of the cementation process [27] and Reaction 4 prevails when the Cu^{2+} ion concentration is low (e.g., at the end of the process).

Concerning the fabrication of the modified polymer electrode, it has been shown [2] that the distribution of the doping metal is a function of the PPy layer thickness for a given amount of deposited metal. It has been found

that the deposition of the metal particles may occur near the PPy surface or can diffuse into the polymer film. When the metal particles are rather located near the surface of the polymer film, the conversion rate of the oxygen and proton reduction is high, because a large metal area is then available for reaction. Conversely, when the metal particles are diluted into the film, they may contact the electrode and therefore decrease the conversion rate for oxygen and proton reduction.

This model of cementation is valid for any system involving a porous deposit. In the large number of basic studies on cementation [14, 15, 17, 29–33], it has been shown using rotating disc electrodes that, in most cases, the reactions are first order and diffusion controlled. However, positive deviations from a first order rate have been observed and two different explanations have been proposed [14, 15, 33]. The rate enhancement can result either from changes in the deposit structure generating increases in the surface area [14, 15], or from the presence of turbulence associated with increasing roughness of the deposit [33]. However, a negative deviation from a first order rate can result from the blocking effect caused by the deposit [34, 35]. It must be also verified that the mixed potential of the system corresponds to iron corrosion, thus avoiding the passivation phenomenon which might result in reducing or blocking the cementation process.

An iron electrode was used in this work and PPy electrodeposition was performed in oxalic acid, following the conditions described by Beck et al. [36]. Then, after the PPy film was formed at the electrode, it was immersed in an aqueous sulphate acidic solution containing Cu^{2+} ion where the cementation process occurred.

The electrochemical response of copper on the 'modified' polymer electrode with respect to the proton discharge is compared to that of the unmodified one and to the metallic copper electrode. The results are explained in terms of the modification of the electrocatalytic properties of the polymer film caused by the incorporation of copper.

2. Experimental details

PPy electrodeposition on iron was performed in 0.1 M oxalic acid and 0.1 M pyrrole (synthesis quality from Merck). Pyrrole was freshly distilled under nitrogen just before use. The reagents were stored at 0 °C in the dark. Electrolytes were dissolved in bidistilled water. PPy electropolymerization was conducted at room temperature, under deaerated atmosphere by bubbling argon and in an unstirred solution. The iron working electrode was a rotating disc of area 0.2 cm². A Tacussel (EDI type) unit controlled the rotation speed, ω . Before each experiment, the working iron electrode was polished with emery papers to 1200 grit and finally rinsed with distilled water. A commercial reference electrode (saturated calomel electrode SCE) placed in a separate compartment containing the supporting electrolyte, and

a platinum auxiliary electrode were used. Cyclic voltammetry and chronopotentiometry experiments were run using a Tacussel PGP201 potentiostat/galvanostat coupled with an HP micro-computer under 'Voltamaster logiciel'. The PPy electrodeposition was performed at constant current densities, and the best results were obtained with a current density of 2 mA cm⁻². Different deposition times were used to produce PPy layers with different thickness and morphologies. The proton reduction on the doped PPy electrode was conducted in 0.1 M Na₂SO₄, H₂SO₄ (pH 1).

The cementation process was carried out using the iron rotating disc so as to determine the reaction kinetics, in a sulphate acidic solution containing Cu^{2+} ions at different initial concentrations (1×10^{-5} , 5×10^{-4} and 10^{-3} M), H₂SO₄ (pH 1) and 0.1 M Na₂SO₄ as supporting electrolyte. Samples of 1 cm³ were removed sequentially for AA analysis. The Cu^{2+} concentration time-dependent was followed during cementation with an atomic absorption spectrophotometer (Shimadzu AA-6500) controlled with a microcomputer. The analysis was conducted with an oxidising air-acetylene flame at 324.7 nm wave length. Also, the PPy film morphology was investigated by scanning electron microscopy (SEM).

3. Results and discussion

3.1. Galvanostatic PPy electrodeposition on iron

Figure 1 shows the potential against time curve obtained at 2 mA cm⁻² for the PPy electropolymerization on iron in oxalic acid. The working electrode potential was at first negative (–500 mV vs SCE) for about 150 s and then suddenly jumped to very high positive values, in the range 600–900 mV vs SCE. The curve showed an induction period. The initial negative potential was ascribed to an active dissolution of iron. Polypyrrole (black and adherent deposit) was electrodeposited at the

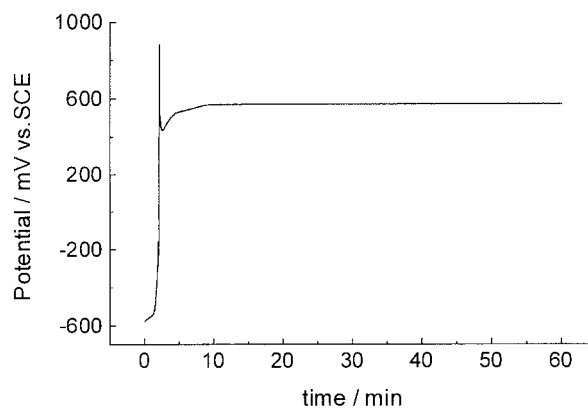


Fig. 1. chronopotentiometry curve for the galvanostatic electrodeposition of polypyrrole (PPy) on iron from aqueous electrolyte (0.1 M pyrrole, 0.1 M H₂C₂O₄), current density $i = 2 \text{ mA cm}^{-2}$. (This electrolysis was conducted under different electrolysis times of 10, 30 and 60 min).

positive potential plateau (600 mV vs SCE). This PPy electrolysis was conducted at different electrolysis times (10, 30 and 60 min) at a constant current density of 2 mA cm^{-2} to obtain different PPy morphologies (variation of porosity and thickness). These different polymer electrodes were then immersed in an acidic sulphate solution containing various initial Cu^{2+} ion concentrations where the cementation process was conducted.

3.2. Rate constant of the cementation process

Cementation of Cu^{2+} ions onto a rotating Fe/PPy electrode (PPy film deposited with an electrolysis time of 60 min) is shown in Figure 2. This Figure shows the variation of $\log(C^\circ/C)$ with cementation time for various rotation speeds (ω) of the Fe/PPy electrode. Terms C° and C denote the initial concentration and the concentration at time t of Cu^{2+} ions, respectively. The curves are linear with two distinct slopes showing: a fast initial rate and a final slower one. Different reaction rates for the cementation processes at metallic electrodes were observed earlier [17, 24, 33, 35, 37–39]. The decrease in the cementation rate at longer reaction times is due [35, 40] to the formation of a solid layer of metallic copper at the surface, closing the pores of the PPy electrode, thus decreasing the reaction rate. Another possible reaction [26], using the thermodynamic approach, is the reduction of ferric ions by the partial redissolution of the copper deposit. This yields cupric and ferrous ions in solution [25, 26].

For the different rotation rates (ω) used and for cementation times not exceeding 10–20 min, $\log(C^\circ/C)$ appears to be proportional to the cementation time t . Following [11, 16–18, 23, 33, 35, 41], it can be written:

$$2.3 \log(C^\circ/C) = (kA/V)t \quad (5)$$

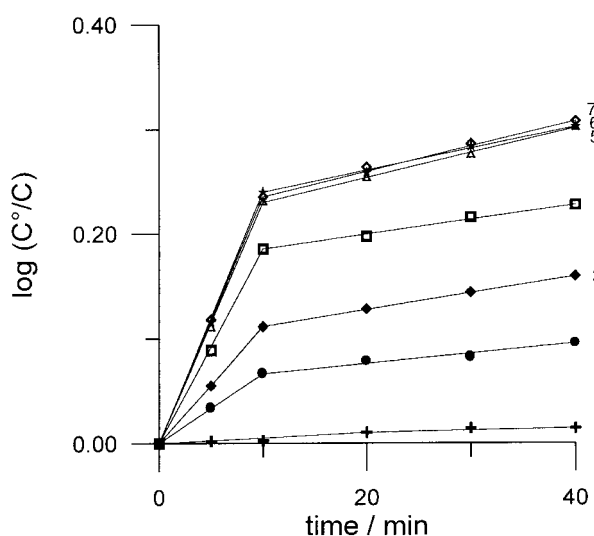


Fig. 2. Cementation time-dependence of $\log(C^\circ/C)$ for various rotation speeds ω (rpm) of the Fe/PPy electrode (PPy obtained with 60 min electrolysis time at 2 mA cm^{-2}). Electrolyte containing $10^{-3} \text{ M Cu}^{2+}$, $0.1 \text{ M Na}_2\text{SO}_4$, H_2SO_4 (pH 1), $T = 25^\circ \text{C}$. ω : (1) 0, (2) 200, (3) 500, (4) 1000, (5) 1500, (6) 2000 and (7) 4000 rpm.

where k is the rate constant for Cu^{2+} ion cementation, referred to the electrode area A and to the electrolyte volume V . From this equation the cementation rate constant k , deduced from the slope of straight lines in Figure 2, is a linear function of the square root of the electrode rotation speed ($\omega < 1500 \text{ rpm}$), as shown in Figure 3, in agreement with a diffusion controlled cementation process. For $\omega > 1500 \text{ rpm}$ the rate constant was found to be independent of stirring. A similar result for copper cementation onto iron was found by Nadkarni et al. [25]. Therefore, at higher stirring rates, a chemical process dominates the kinetics.

The stoichiometry of Equation 1 indicates a molar ratio of unity for iron consumed per mole of recovered copper. Thus, an analysis of the Fe^{2+} ion concentration in solution during cementation was performed at different rotation speeds (see Figure 4). At any rotation

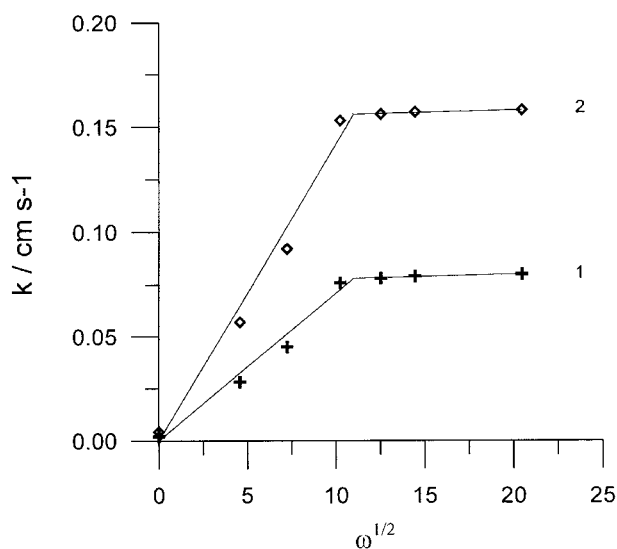


Fig. 3. Variation of the cementation rate constant k with the electrode rotation speed. Conditions as in Figure 2. Key: (1) $\text{Cu}^{2+} = 5 \times 10^{-4} \text{ M}$; (2) $\text{Cu}^{2+} = 10^{-3} \text{ M}$.

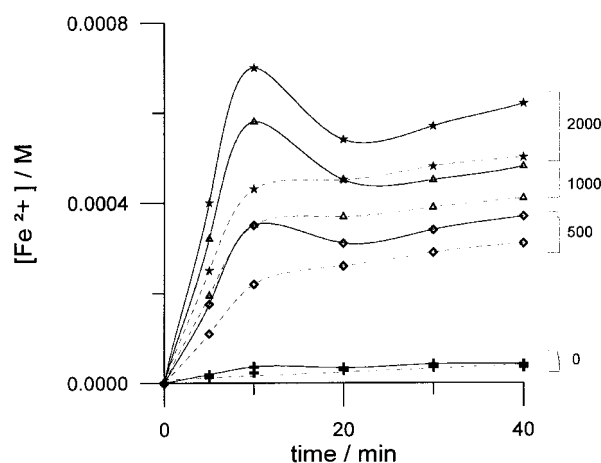


Fig. 4. Fe^{2+} ions concentration in the cell produced during cementation with varying the electrode rotation speed. Conditions as in Figure 2. Key: (----) under stoichiometric conditions; (—) our experimental results.

speed, the cementation reaction produces excess iron above that stoichiometrically required for copper cementation. Iron dissolves 1.6 times faster than the stoichiometric conditions at the beginning and 1.2 times faster at the end of the reaction.

3.2.1. Effect of the PPy deposit morphology on the cementation reaction rate

Figure 5 shows the variation of $\log(C^\circ/C)$ with the cementation time for various C° values. The Fe/PPy electrodes used are obtained with different electrolysis times of 10, 30 and 60 min. For different C° (1×10^{-5} , 5×10^{-4} and 1×10^{-3} M) and for cementation time not exceeding 10–20 min, it appears that for the different electrodes, the rate constant, k , of the process deduced from the slope of the straight lines in Figure 5 increases both with increasing C° and PPy electropolymerization charge. These results are not in accordance with a true first order reaction which normally implies that the rate constant should be independent of the initial concentration C° . These changes of k against C° are widely accepted in the literature [15–18, 25, 31, 41–43] and ascribed to variations in the electrode area due to the copper deposit irregularities and to the iron corrosion. Figure 6 summarizes the results for the variations of k with both C° and PPy electropolymerization charge. Figure 6 also shows that the percentage recovery of cupric ions from solution increased with increasing C° or PPy electropolymerization charge.

As an example, the corresponding Fe/PPy potential change during cementation, for $C^\circ = 10^{-3}$ M and $\omega = 1000$ rpm, is shown in Figure 7. The bare iron electrode potential evolution during cementation is also presented in the same figure. During cementation, the electrode used (PPy or iron) is progressively covered by a metallic copper deposit; then for comparison, the copper equilibrium potential variation in the same solution at a constant C° (1×10^{-3} M) of Cu^{2+} is also reported. It can be seen that the PPy working electrode potential is at first positive (around +400 mV vs SCE) and becomes more negative until some steady state value is reached after 10–20 min. At zero time, the recorded potential is the 'equilibrium' potential of the PPy film in solution. It can be seen that this 'equilibrium' potential (+400 mV vs SCE) is more positive than the metallic copper equilibrium potential (around 10 mV vs SCE in 10^{-3} M Cu^{2+}). When the cementation process occurs, the concentration of Cu^{2+} in solution decreases with the cementation time and the PPy electrode surface is partially covered by metallic copper, scheme 1. This potential decrease during cementation is probably due to (i) the formation of a new (PPy + Cu) electrode where the potential is less positive than the PPy electrode (ii) the decrease in Cu^{2+} concentration with cementation time.

The higher steady state potential value corresponds to the higher electrolysis time (60 min) for the PPy electrode. In this case, the increased roughness of the PPy film and, therefore, the larger reactive surface area

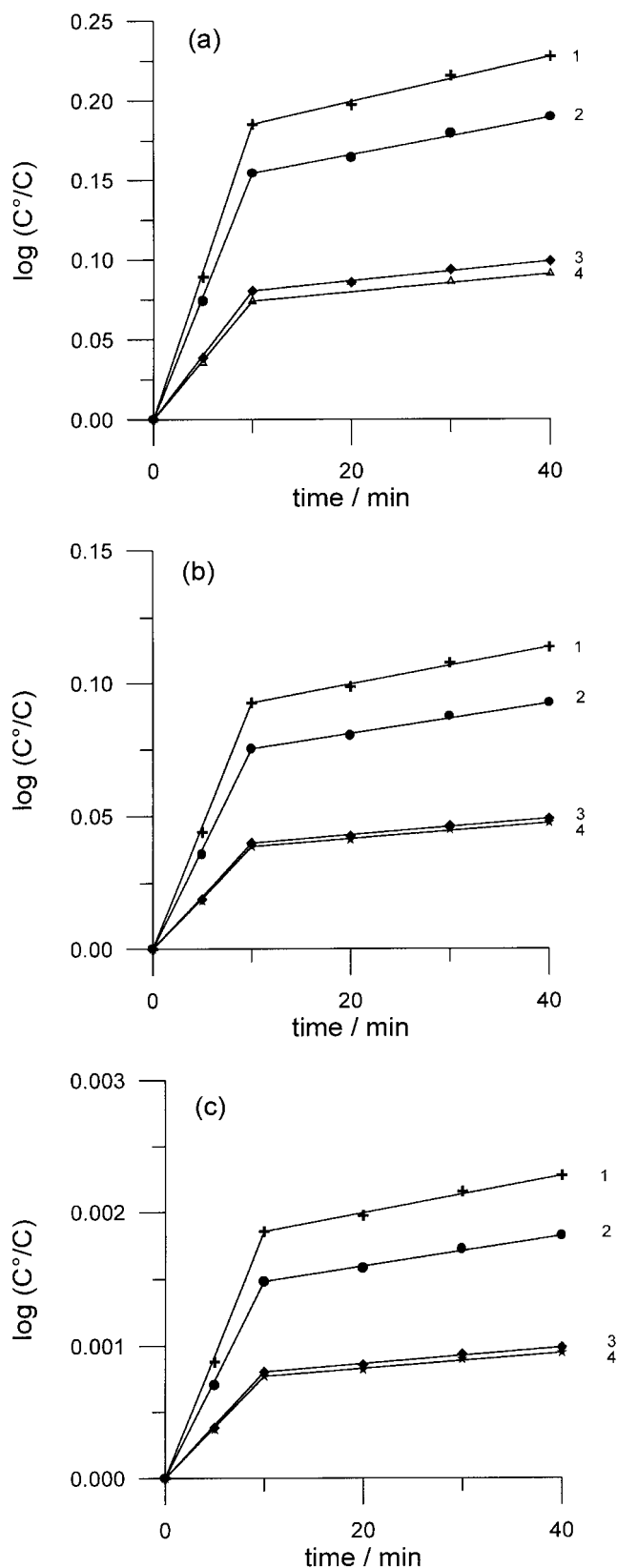


Fig. 5. Cementation time-dependence of $\log(C^\circ/C)$ for various initial Cu^{2+} concentration C° , $\omega = 1000$ rpm, 0.1 M Na_2SO_4 , H_2SO_4 (pH 1), $T = 25^\circ\text{C}$. Key: for Cu^{2+} : (a) 1×10^{-3} , (b) 5×10^{-4} and (c) 1×10^{-5} M. Using different PPy films obtained at different electrolysis times of (1) 60, (2) 30 and (3) 10 min; (4) bare iron electrode.

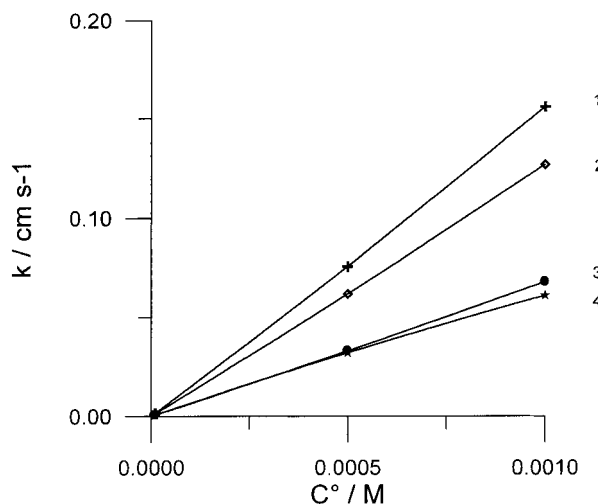


Fig. 6. Variation of the cementation rate constant k (cementation time 10–20 min) with the initial Cu^{2+} ions concentration using PPy electrodes obtained at various electrolysis times. Conditions as in Figure 5. Times: (1) 60, (2) 30 and (3) 10 min; (4) bare iron electrode. (Figure deduced from the slope of the straight lines of the Figure 5).

enhances the cementation reaction rate and the PPy electrode is mainly covered with metallic copper. The electrode potential is shifted to more positive values approaching the copper metal electrode potential but remains below that of a copper electrode because the Cu^{2+} concentration is low (the copper electrode potential evolution presented in Figure 7, (curve 5) is relative to a constant Cu^{2+} concentration (10^{-3} M). These results mean that the copper ion recovery by cementation is more efficient using the PPy electrode prepared with a high electrolysis time (60 min). These results are in good agreement with those obtained in the kinetic study of the cementation reaction (Figures 5 and 6).

The evolution of the open circuit potential (OCP) of the Fe/PPy electrode without Cu^{2+} in the same electrolyte is presented in Figure 8. Comparison of the OCP evolution without Cu^{2+} and with Cu^{2+} would provides

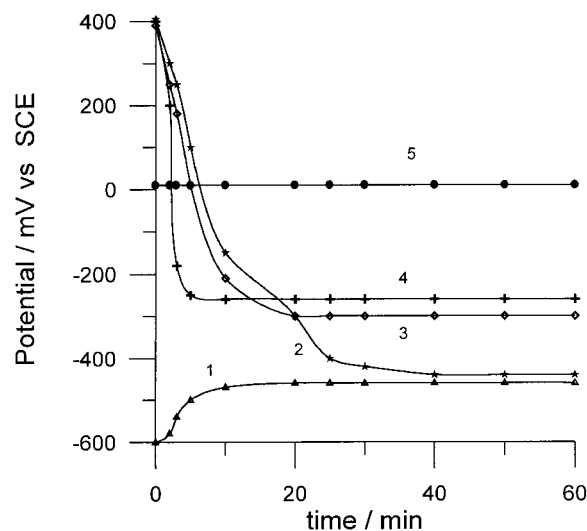
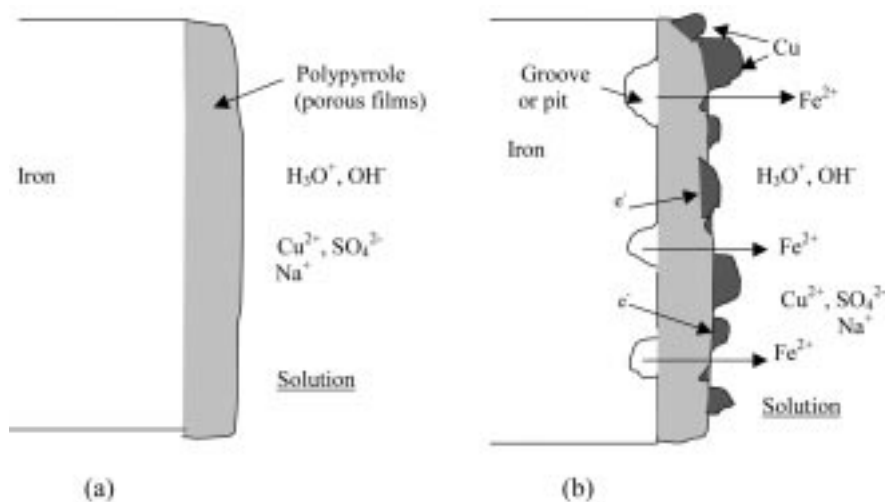


Fig. 7. Potential evolution during the cementation process with different PPy films obtained at different electrolysis times. Solution containing 10^{-3} M Cu^{2+} , 0.1 M Na_2SO_4 , H_2SO_4 (pH 1), $T = 25^\circ\text{C}$, $\omega = 1000$ rpm. Key: (1) bare iron electrode, (2) 10 min, (3) 30 min, (4) 60 min and (5) bare metallic copper electrode at constant Cu^{2+} concentration (10^{-3} M).

evidence about the cementation process on the film: if Cu^{2+} exchanges electrons with PPy, this would slow down the evolution of the OCP; if Cu^{2+} exchanges electrons directly with the iron substrate this would accelerate the return to active dissolution.

The starting value of corrosion potential (about +400 mV vs SCE) corresponds to the potential of the redox process in the PPy film. The corrosion potential becomes stable after about 70 min for the electrode coated at the higher electrolysis time (60 min). This was close to the corrosion potential of bare iron in the same solution (around -600 mV vs SCE). The same results were found in [44] in the case of the corrosion protection of mild steel by PPy coatings in acid sulphate. This OCP



Scheme 1. Diagram showing the morphology change from polypyrrole covered electrode (a) to the deposit of copper covered surface at time t of cementation (b). The possible reactions mechanisms involved in the cementation process.

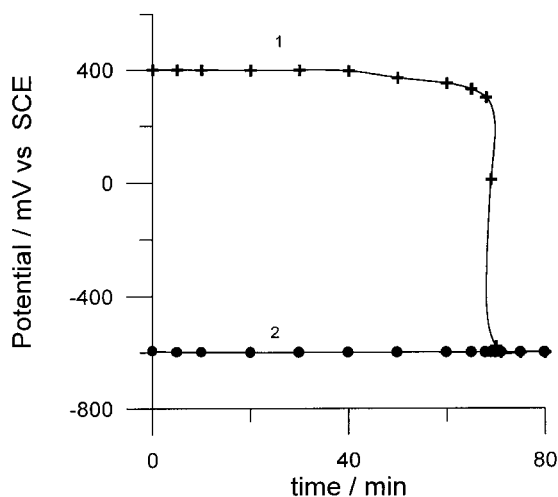


Fig. 8. Evolution of the open circuit potential (OCP) with time in 0.1 M Na₂SO₄, H₂SO₄ (pH 1), $T = 25\text{ }^{\circ}\text{C}$, $\omega = 1000\text{ rpm}$. (1) For PPy coated iron after electropolymerization at 2 mA cm^{-2} , electrolysis time 60 min; (2) for bare iron electrode.

behaviour substantiates the electron exchange between copper and PPy during the cementation process.

3.3. Microscopy of a PPy film containing Cu microparticles

To confirm the presence of Cu particles in the PPy film, SEM coupled with EDX analysis was performed. As observed in Figure 9, the PPy deposit presents a grained texture and must be compared with the much coarser cauliflower structure which is commonly found [45, 46]. The copper particles appear as small bright spots, Figure 10. A large amount of embedded Cu particles is visible with a uniform distribution.

An EDX analysis of the PPy film containing Cu microparticles, Figure 11, conducted with a fine electron beam, again confirmed the presence of copper on the PPy film. Iron and sulphur were also detected, due to the substrate and to the SO₄²⁻ anions.

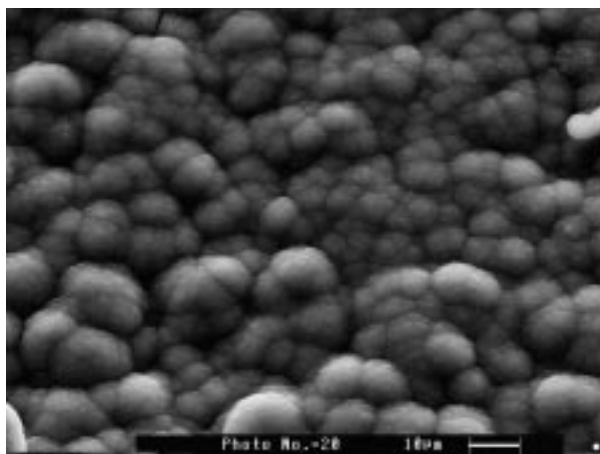


Fig. 9. SEM surface micrograph of a PPy film obtained on iron in 0.1 M pyrrole and 0.1 M H₂C₂O₄, in galvanostatic conditions (2 mA cm^{-2}) and electrolysis time 60 min.

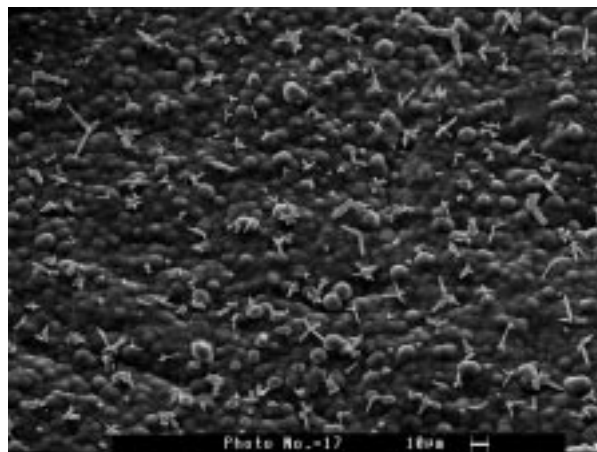


Fig. 10. SEM surface micrograph of PPy/Cu modified electrode by using cementation process during 40 min in 10^{-3} M Cu^{2+} , 0.1 M Na₂SO₄, H₂SO₄ (pH 1), $T = 25\text{ }^{\circ}\text{C}$, $\omega = 1000\text{ rpm}$ (copper particles appear as bright spots).

3.4. Polarization curves of copper-containing polypyrrole electrodes against the proton reduction

The proton reduction in an acidic sulphate solution of 0.1 M Na₂SO₄ and H₂SO₄ (pH 1) was studied as a method of determining the electrochemical response of the copper-containing polypyrrole electrodes obtained at different electrolysis and cementation conditions and to compare their behaviour with that of a copper electrode.

The catalysis of slow reactions at the surface of redox film modified electrodes is affected essentially by (i) the intrinsic reactivity of the catalyst (Cu, in this case), (ii) the rate of the catalytic reaction between the catalyst and substrate (H⁺ in this case), (iii) the rate of permeation of substrate into the film and the rate of electron transport through the film, and (iv) the rate of diffusion of the substrate from the bulk of the solution to the film-surface interface [47, 48]. Moreover, two or more of these factors may act simultaneously.

Figure 12 shows the polarization curves for proton reduction ($2\text{H}^{+} + 2\text{e}^{-} \rightarrow \text{H}_2$) at pH 1, for the polypyrrole electrode and polypyrrole modified with copper. The polypyrrole layer, in this case, was obtained after an electrolysis time of 60 min at 2 mA cm^{-2} , and was cemented for 40 min with different initial Cu²⁺ concentrations (1×10^{-5} , 5×10^{-4} , $1 \times 10^{-3}\text{ M}$). Figure 12 shows that the rate of hydrogen evolution increases when cementation is performed at high initial Cu²⁺ concentrations. The polarization curve for hydrogen evolution conducted with the cemented electrode in a 10^{-3} M Cu^{2+} solution is near that for the metallic copper electrode. This means that this modified electrode is uniformly covered with metallic copper. This result is in good agreement with those obtained above, where it is shown that the copper recovery by cementation increases with initial increasing Cu²⁺ concentration. When modified Cu-polypyrrole electrodes are obtained by cementation with a constant initial Cu²⁺ concentration

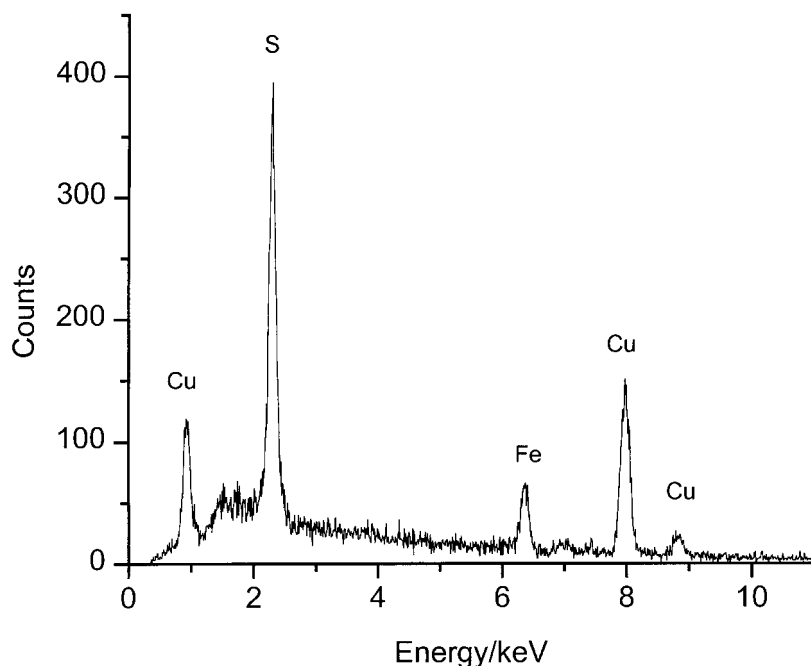


Fig. 11. EDX analysis of the PPY/Cu surface (experiment coupled with SEM analysis of Figure 10).

and with different polymer film morphologies (obtained at different electrolysis times of 10, 30 and 60 min) the proton discharge in this case shows also that the more catalytic modified electrode against the reduction of H^+ is that obtained with higher electrolysis time of 60 min (Figure 13). This behaviour is due to the increase in metallic copper incorporation in the polymer film with increase in polypyrrole film thickness. This confirms the results obtained above showing the increase in copper recovery by cementation by using a thicker polypyrrole layer (Figures 5 and 6).

The electrocatalytic behaviour of these modified electrodes containing dispersed Cu particles with respect to methanol oxidation [49, 50], hydrazine oxidation [51], characterization of their thermal properties by thermogravimetric analysis [52] and investigation by impedance

spectroscopy of redox processes occurring at this modified electrode [53] are under study in our laboratory.

4. Conclusion

The first results of this work showed that the modification of a conducting polypyrrole film by the deposition of metallic copper particles using electrochemical cementation can be achieved. Cementation experiments were performed over a large range of copper ion initial concentrations and using different polymer layer thicknesses. The copper-polypyrrole modified film deposited at an iron electrode acts as an electrocatalyst for the proton reduction. The catalytic current is dependent on

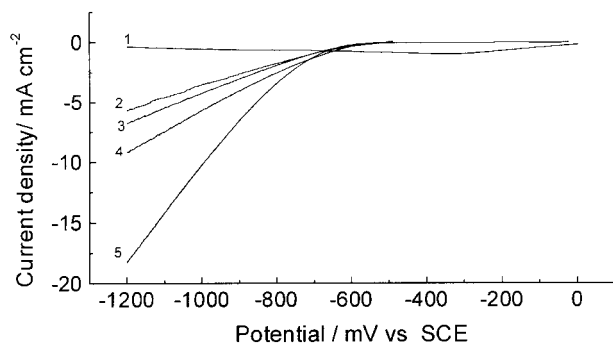


Fig. 12. Polarization curves of Cu-modified PPY electrodes vs. the proton reduction in 0.1 M Na_2SO_4 , H_2SO_4 (pH 1), $T = 25^\circ C$, $\omega = 1000$ rpm. Modified electrodes were obtained after 40 min of cementation at various initial Cu^{2+} ions concentrations: (1) PPY, (2) 1×10^{-5} M, (3) 5×10^{-4} M, (4) 1×10^{-3} M and (5) bare metallic copper.

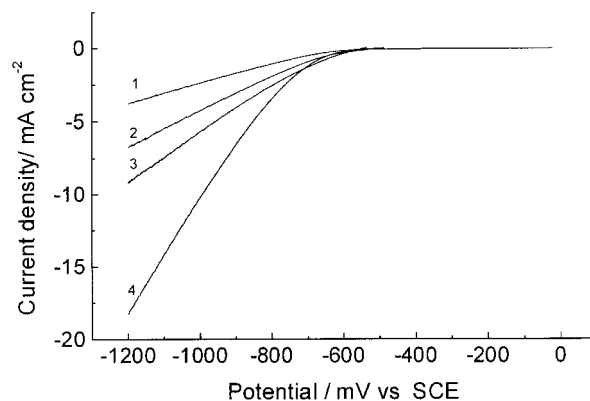


Fig. 13. Polarization curves of Cu-modified PPY electrodes vs. the proton reduction in 0.1 M Na_2SO_4 , H_2SO_4 (pH 1), $T = 25^\circ C$, $\omega = 1000$ rpm, by using polymer films electrodeposited at different electrolysis times: (1) 10, (2) 30 and (3) 60 min; (4) bare metallic copper electrode. (Modified electrodes were obtained after 40 min of cementation with 10^{-3} M Cu^{2+}).

the cementation process of the modified electrode, notably the variation in the initial Cu^{2+} concentration and the variation of the polymer deposit morphology. The electrochemical response of these electrodes showed higher currents for proton reduction as compared to 'unmodified' polymer electrodes.

Acknowledgements

B. Saidani acknowledges the I.D.B bank, Saudi Arabia, for financial support.

References

1. A. Galal, *J. Solid. State Electrochem.* **2** (1998) 7.
2. A. McGee, J.F. Cassidy, P. Quigley and J.G. Vos, *J. Appl. Electrochem.* **22** (1992) 678.
3. C.S.C. Bose and K. Rajeshwar, *J. Electroanal. Chem.* **333** (1992) 235.
4. R.A. Bull, F.R. Fan and A.J. Bard, *J. Electrochem. Soc.* **130**(7) (1983) 1636.
5. M.E.G. Lyons, *Analyst* **119** (1994) 805.
6. S.A. Emr and A.M. Yacynych, *Electroanalysis* **7** (1995) 10.
7. M. Josowicz, *Analyst* **120** (1995) 1019.
8. C. De la Fuente, J.A. Acuna, M.D. Vasquez, M.L. Tascon, M.I. Gomez and P. Sanchez Batanero, *Talanta* **44** (1997) 685.
9. I. De Gregori, M. Carrier, A. Deronzier, J.C. Moutet, F. Bedioui and J. Devynck, *J. Chem. Soc. Faraday Trans.* **88** (11) (1992) 1567.
10. J.C. Moutet, A. Zouaoui, O. Stephan and M. Carrier, Journées d'Electrochimie de Toulouse (France), 1–4 juin (1999) CA–2.1.
11. G.P. Power and I.M. Ritchie, *Aust. J. Chem.* **29** (1976) 699.
12. J.T.T. Pang and I.M. Ritchie, *Electrochim. Acta* **27** (1982) 683.
13. C.C. Kenna, I.M. Ritchie and P. Singh, *Hydrometallurgy* **23** (1990) 263.
14. W.Y. Wei, C. Lee and H.J. Chen, *Langmuir* **10** (1994) 1980.
15. G. Puvvada and T. Tran, *Hydrometallurgy* **37** (1995) 193.
16. L. Makhloufi, Doctorat thesis, Grenoble (France) (1987).
17. L. Makhloufi, S. Bourouina and S. Haddad, *Electrochim. Acta* **37**(10) (1992) 1779.
18. L. Makhloufi, B. Saidani, C. Cachet and R. Wiart, *Electrochim. Acta* **43**(21–22) (1998) 3159.
19. L. Makhloufi, B. Saidani and H. Hammache, *Wat. Res.* **34**(9) (2000) 2517.
20. L. Makhloufi and B. Nguyen, *J. Soc. Alger. Chim.* **8**(2) (1998) 141.
21. M.E. Wadsworth, *Trans. Met. Soc. AIME* **245** (1969) 1381.
22. M.E. Wadsworth and J.D. Miller, in H.Y. Sohn, and M.E. Wadsworth (Eds), 'Hydrometallurgical Process' (Plenum, New York, 1979), p. 197.
23. W.W. Fisher, *Hydrometallurgy* **16** (1986) 55.
24. L. Makhloufi, B. Saidani and L. Dimanova, *Izv. Vyssh. Uchebn. Zaved.*, vol. 5 (ISSN 0363-0797 Moscow, 1996), p. 7.
25. R.M. Nadkarni, C.E. Jelden, K.C. Bowles, H.E. Flanders and M.E. Wadsworth, *Trans. Met. Soc. AIME* **239** (1967) 581.
26. R.S. Rickard and M.C. Fuerstenau, *Trans. Met. Soc. AIME* **242** (1968) 1487.
27. M. Foulletier, J.B. Mathieu and P. Noual, 'Les Applications de l'Electrochimie à l'Hydrometallurgie' (Ed. Pluralis, Paris, 1980), p. 129.
28. R.M. Nadkarni and M.E. Wadsworth, 'Advances in Extractive Metallurgy' (Institution Mining Metallurgy, London, 1968, p. 918.
29. N. Massé and D. Piron, *J. Electrochem. Soc.* **140** (1993) 2818.
30. J. Zheng, M. Khan, S.R. La Brooy, I.M. Ritchie and P. Singh, *J. Appl. Electrochem.* **26** (1996) 509.
31. K. Zaghib, E. Chainet and B. Nguyen, *Electrochim. Acta* **35**(3) (1990) 657.
32. C. Alemany, J.P. Diard, B. Le Gorrec and C. Montella, *Electrochim. Acta* **41**(9) (1996) 1483.
33. I.M. Ritchie and S.G. Robertson, *J. Appl. Electrochem.* **27** (1997) 59.
34. A. Fontana, J. Martin, J. Van Severen and R. Winand, *Metallurgie* **XI**(3) (1971) 168.
35. Y.A. El-Tawil, *Z. Metallkde. Eingegangen am* **26** (1987) 544.
36. F. Beck, R. Michaelis, F. Schlöten and B. Zinger, *Electrochim. Acta* **39**(2) (1994) 229.
37. G.P. Power and I.M. Ritchie, *Proc. Electrochemistry Division* (1975) 39.
38. R.M. Morrison, D.J. Mackinnon and J.M. Brannen, *Hydrometallurgy* **18** (1987) 207.
39. E.C. Lee, F. Lawson and K.N. Han, *Hydrometallurgy* **3** (1978) 7.
40. R.M. Nadkarni and M.E. Wadsworth, *Trans. Met. Soc. AIME* **239** (1967) 1066.
41. K. Zaghib, E. Chainet and B. Nguyen, *J. Electrochem. Soc.* **144**(11) (1997) 3772.
42. J.P. Gould, I.B. Escovar and B.M. Khudenko, *Wat. Sci. Tech.* **19** (1987) 333.
43. J.D. Miller and L.W. Beckstead, *Metallurgical Transactions* **4** (1973) 1967.
44. N.V. Krastajic, B.N. Grgur, S.M. Jovanovic and M.V. Vojnovic, *Electrochim. Acta* **42**(11) (1997) 1685.
45. F. Beck and M. Oberst, *Macromol. Chem.* **8** (1987) 97.
46. W. Su and J.O. Iroh, *J. Appl. Polym. Sci.* **65**(3) (1997) 417.
47. C.P. Andrieux and J.M. Saveant, *J. Electroanal. Chem.* **134** (1982) 163.
48. C.P. Andrieux, J.M. Dumas-Bouchiat and J.M. Saveant, *J. Electroanal. Chem.* **31** (1982) 1.
49. M. Gholamian and A.Q. Contractor, *J. Electroanal. Chem.* **289** (1990) 69.
50. K. Shimazu, R. Inada and H. Kita, *J. Electroanal. Chem.* **284** (1990) 523.
51. S.M. Golabi and F. Noor-Mohammadi, *J. Solid State Electrochem.* **2** (1998) 30.
52. S. Mokrane, L. Makhloufi, H. Hammache and B. Saidani, *J. Solid State Electrochem.* (Springer Ed., 1999), (submitted to publication).
53. C. Deslouis, M.M. Musiani and B. Tribollet, *J. Chim. Phys.* **86**(1) (1989) 205.
54. C. Deslouis, M.M. Musiani and B. Tribollet, *J. Electroanal. Chem.* **269** (1989) 57.